

PHYSICAL METALLURGY OF ACICULAR FERRITE FORMATION

FYZIKÁLNÍ METALURGIE VZNIKU ACIKULÁRNÍHO FERITU

Authors: Doc. Ing. Eva Mazancová, CSc., Prof. Ing. Zdeněk Jonšta, CSc., Prof. RNDr. Petr Wyslych, CSc., Prof. Ing. Karel Mazanec, DrSc.*

*Working place: Department of Materials Engineering, *Department of Physics, Faculty of Metallurgy and Materials Engineering, Technical University of Ostrava*

Address: 17. listopadu 15, 708 33 Ostrava-Poruba, Czech Republic

Telephone: [420/596994409](tel:420596994409)/ e-mail: eva.mazancova@vsb.cz, zdenek.jonsta@vsb.cz, petr.wyslych@vsb.cz

Abstract

The work concerns the analysis of physical metallurgy acicular ferrite characteristics. Acicular ferrite is nucleated intragranularly on the non-metallic inclusions unlike the intergranularly initiated upper bainite. Acicular ferrite microstructure is characterised by predominant occurrence of high-angle interface.

Práce je věnována rozboru fyzikálně metalurgických charakteristik acikulárního feritu. Ten je nukleován intragranulárně na nekovových inkluzích na rozdíl od intergranulárně iniciovaného horního bainitu. Mikrostruktura acikulárního feritu je charakterizována převážně velkoúhlovým rozhraním desek.

Key words

acicular ferrite, high-angle boundary, interfacial energy, non-metallic inclusions

ferit acikulární, hranice velkoúhlová, energie fázového rozhraní, inkluze nekovové

Introduction

It is generally accepted that the mechanism controlling the austenite (A) decomposition into acicular ferrite (AF) is identical to the mechanism controlling the formation of upper bainite (B) microstructure. The difference among transformation products consist in the distinct initiation sources. The main difference arises in the side at which each microstructure nucleates. The B is nucleated at A-grain boundaries and/or at active interface of allotriomorphic ferrite (ATF) with A [1], the AF plates are intragranularly nucleated at non-metallic inclusions present in the steel matrix. As the AF nucleating non-metallic inclusions act the particles fulfilling the specific physical and chemical conditions [2].

Physical metallurgy of AF nucleating process

Previously performed investigations concerning the AF formation principles have led to the elucidation of influence concerning the A-reduction grain boundary surfaces per unit of volume. This favours the AF initiation process in comparison with the effect connected with upper B formation. The consequence of this process is a decrease in the number of B potential nucleations sites. The similar effect can be detected if the higher density of potential non-metallic inclusions is present in steel [3]. The increased AF volume fraction can be also achieved if an intergranularly nucleated ATF in the form of thin layers „decorating“ a grain-boundaries is inert what e.g. limits the continuous Widmanstätten ferrite (WF) formation. The cause of considered limiting effect is the carbon partitioning into A at A/F interface providing that local carbon concentration is large enough to depress the start of WF and/or B initiation during the subsequent A-decomposition [1]. Figure 1 shows the inert ATF/A-interface and AF formation in A-grain volume. On the contrary, Fig.2 presents the development of continuously growing WF from the ATF layer as it results from the ATF/A active interface behaviour.

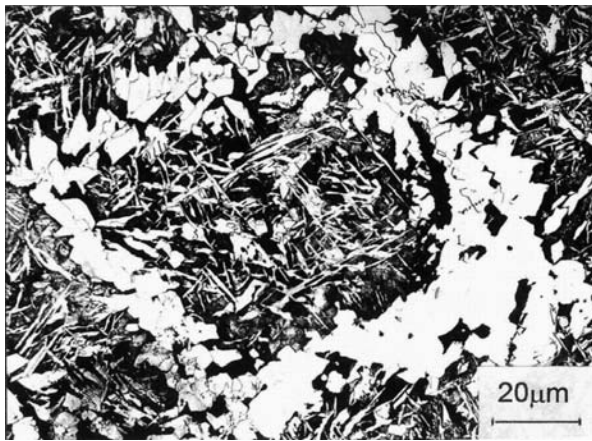


Fig. 1. AF-microstructure, influence of inert ATF-interface with A

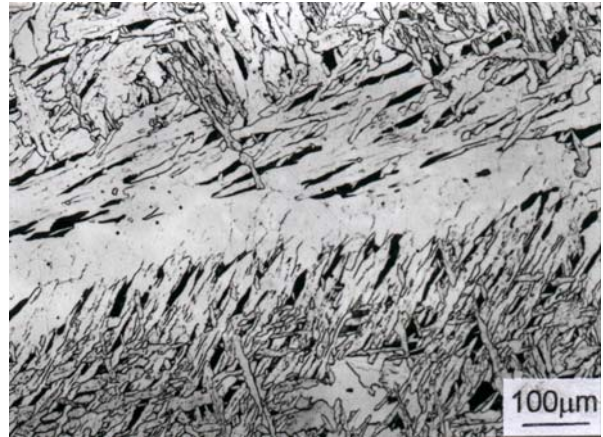


Fig.2 ATF and side plate ferrite (WF) microstructure

Several mechanisms have been proposed to explain the way how non-metallic inclusions favour the AF nucleation. Even though the limited number of steels containing effective oxides particles being available yet, the results obtained so far for Ti-deoxidized steels are encouraging and demonstrate the hopeful AF intragranular nucleation [4]. In such attempts, it must be well understood which phase detected at usually heterogeneous non-metallic inclusions (adhered at „bearing“ non-metallic inclusions) is more effective for intragranular nucleation process. In this connection, with respect to simultaneous knowledge level, four variants can be taken into consideration: 1) simple heterogeneous nucleation on an inert particle, 2) epitaxial nucleation on the inclusion having a good lattice registry (coherency) with ferritic particles, 3) nucleation arising from the strain energy associated with the different thermal expansion coefficients of the inclusions in steel matrix, 4) nucleation connected with solute depletion in matrix near inclusion [5]. It depends on the chemical composition and structural characteristics that which mechanism would worth to promote the intragranular nucleation on inclusion. The Ti_2O_3 inclusion represents an example of a very important

particle contributing to the preferential AF nucleation [3]. This effect is given due to development of local Mn-depletion zone around this inclusion and due to corresponding increase of local chemical free enthalpy, the AF-formation is initiated [5, 6].

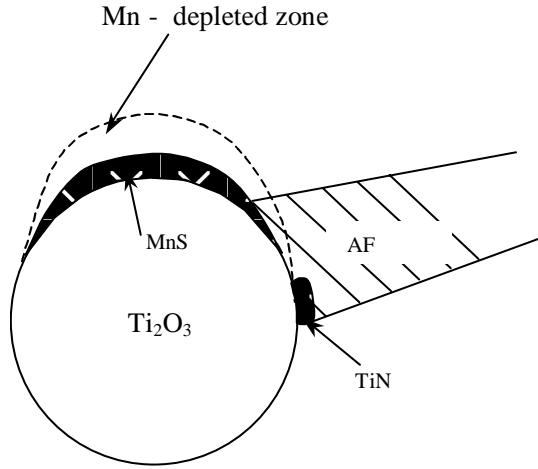


Fig. 3. Schematic illustration of inclusions in steel deoxidized with Ti

The heterogeneity and/or complexity of some inclusions play very interesting role because it makes possible to attain manifold AF-nucleation activity. One way is given by the matrix chemistry modification resulting in solute atoms depletion. The creation of low energy surfaces between AF and A-particles with existence of a beneficial lattice matching between these phases represents the second variant of preferential AF-formation. The realisation of this mechanism is enhanced when a high energy interface between A and inclusion is replaced by a low-energy interface between AF-plates and considered non-metallic particles (see Fig.3 representing a basic Ti_2O_3 variant with adhered MnS and TiN).

Analysis of AF initiation process

The observed microstructure results have been interpreted using classical heterogeneous nucleation theory [7]. According to this theory, when the integral energetic balance for the decomposition process of A into AF is evaluated in the case of heterogeneous nucleation at non-metallic inclusions, it is necessary to take into account the next four parameters being included in the following equation:

$$\Delta G_{het} = - (\Delta G_V - \Delta G_S) \cdot V_F + \gamma_{F/A} \cdot S_{F/A} + \gamma_{F/I} \cdot S_I - \gamma_{A/I} \cdot S_I. \quad (1)$$

The first term in this equation represents the decrease of the free enthalpy due to the bulk transformation from A into same ferrite volume V_F , ΔG_V corresponds to the driving force per unit volume of AF transformation. The ΔG_S term is strain energy per unit volume AF. The next two terms represent the increase in free enthalpy due to formation of two new interfaces, F/A and F/I with $\gamma_{F/A}$ and $\gamma_{F/I}$. The last term corresponds to the disappearance of the interface between A and inclusion (I), where interfacial energy per unit area is $\gamma_{A/I}$. This is a negative contribution reducing the integral energy balance. The respective areas of the interfaces are indicated as S_I and $S_{F/A}$ in eq. (1) [8].

The presented solution is based on an assumption that the inclusion does not cause local changes in the matrix composition. As it has been found recently, this assumption is not to the full realised because due to the inclusion the local changes in the matrix chemical composition are observed. The Mn-depletion zone is realised both due to MnS adhering on Ti_2O_3 inclusion and due to direct Mn-diffusion in Ti-oxide inclusion. This process is result of higher cation vacancies concentration in Ti_2O_3 in comparison with their concentration in steel (iron) matrix [3, 9]. The second term associated with the A/AF interface is considered to be independent of the nature of the inclusions. The last two terms in eq. (1) are influenced by the

type of particles on which AF-plates are nucleated and by misfit across the interface with both ferritic and austenitic phases ($\gamma_{F/I}$, $\gamma_{A/I}$). The solution of eq. (1) in the case of nucleation at second phase spherical particles gives the following expressions for the evaluation of critical radius R^* and the energy barrier for nucleation ΔG^*_{het} [7]:

$$R^* = 2 \cdot \gamma_{F/A} / \Delta G_V \quad (2)$$

$$\Delta G_{het} = \frac{1}{2} \cdot \Delta G^*_{hom} [1 + \cos^3 \theta + (I/R)^3 \cdot (2 - 3 \cos \varphi + \cos^3 \varphi) - 3/2 \cdot \sigma \cdot (I/R^*)^3 \cdot (1 - \cos \varphi)], \quad (3)$$

where the angles θ and φ are indicated in the scheme plotted in Fig.4, I is the inclusion radius and

$$\sigma = (\gamma_{A/I} - \gamma_{F/I}) / \gamma_{F/A}. \quad (4)$$

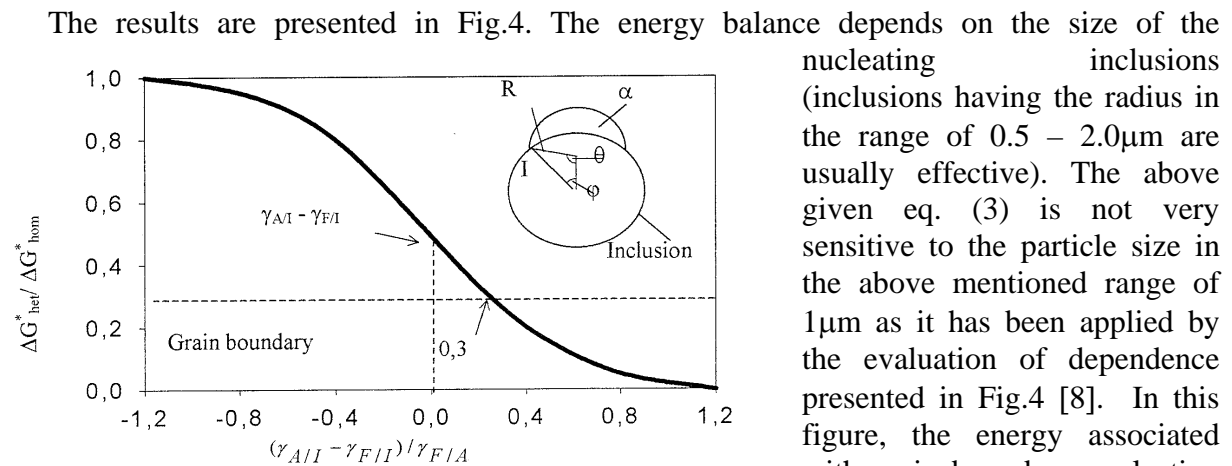


Fig.4. Energy barrier with heterogeneous nucleation and effect of interfacial energy characteristics

As can be seen, when no difference between the interfacial energies $\gamma_{A/I}$ and $\gamma_{F/I}$ is assumed, grain boundary side plate B nucleation is realised with a high frequency. Figure 4 further demonstrates AF-nucleation at inclusions taking part in this process with a high probability when parameter σ (eq. (4)) is greater than 0.3 approximately.

The applied heterogeneous nucleation theory makes possible to describe the physical metallurgy conditions leading to the AF-initiation in A-matrix. The presented analysis confirms that the improvement in the energy balance controlling the development of A-decomposition in AF can be found when a high interface energy $\gamma_{A/I}$ is replaced by a low energy $\gamma_{AF/I}$. The nucleation process is also favoured by the modification of matrix chemistry around inclusions as it results from the interaction: inclusion (considered complex type) – steel matrix. The A in the formed solute atoms depletion zone has increased chemical free enthalpy.

Evaluation of plates misorientation in AF microstructure

The resistance to cleavage fracture in AF microstructure depends on misorientation level of plates. The useful results concerning the misorientation level can be obtained by the application of EBSD technique which makes possible to evaluate the local crystallographic properties of AF microstructure [10, 11]. The evaluation of AF-plates misorientation angles has shown that the most boundaries correspond to the high angle boundaries while the small misorientation ones ($<15^\circ$) have been mainly formed in the space between high angle boundaries. This conclusion results from the determined misorientation map of AF microstructure [10]. The most evaluated high angle boundaries show the misorientation angles higher than 45° approximately [11]. The set of measured misorientation angles in upper B microstructure has confirmed the different level of this value in comparison with AF-microstructure. In this case, the proportion of low-angle boundaries is markedly higher than is found in AF. The distance between the high-angle boundaries in AF is $3\text{-}5\mu\text{m}$ on the average. The distances between the high angle boundaries are $15\text{-}20\mu\text{m}$ approximately what correspond to lower density of effective hindrance for cleavage crack propagation in B-microstructure. The high-angle misorientation can be detected at grain boundaries of B-packets. The density of high crystallography misoriented plates in AF is enhanced by a profuse direct nucleation on non-metallic inclusion particles. In this case it does not seem possible to relate the morphological packet to the microstructure unit which controls the cleavage crack propagation in B-microstructure. The considered unit can be directly related to the set of AF-plates enclosed by high-angle boundaries [11].

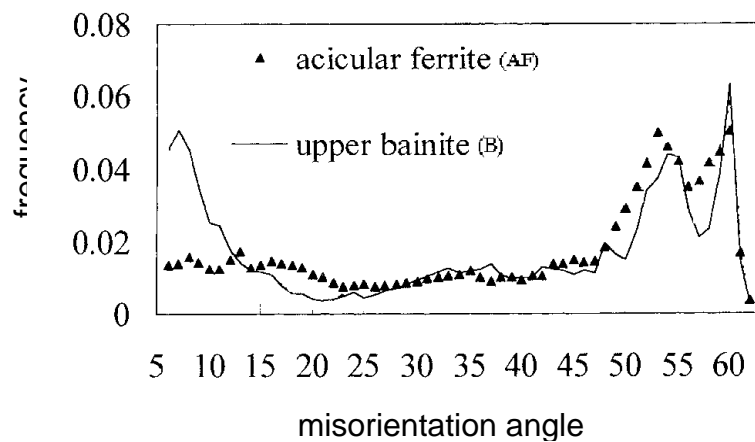


Fig. 5. Histogram of experimental misorientation angle distribution-comparison of AF with upper B [10]

The unit crack path (UCP) corresponds to the distance between the high-angle boundaries and is defined as a region in which the crack propagates in straight line (without detected deviation in growth). The deflection in brittle crack propagation is detected only when the misorientation attains the level of $10\text{-}15^\circ$ (between $\{100\}$ cleavage planes of adjoining plates). Figure 5 shows the histogram of plate misorientation found in AF-microstructure. The dependence detected in upper B-microstructure is presented in this figure for comparison the resistance level of given microstructure to brittle crack formation (plotted the frequency of

measured value in dependence on misorientation angle). In the range of 20-47° approximately a very low frequency of misorientation has been observed. These results follow from the crystallography of realised displacive mechanisms by A-decomposition [10]. The ductile-brittle transition temperature T is usually expressed as being inversely proportional to the root square of distance between high-angle boundaries. The parameters of this process depend on the microstructural characteristics of investigated steel type. The density of crystallographic misorientation planes is enhanced in AF in comparison with B (Fig.5). For this reason the observed AF-microstructure is beneficial due to a higher probability in ascertainable brittle crack deflection than is found in upper B-microstructure [10, 11]. The following type of dependence has been used to decrease the transition temperature in studied steel:

$$T = T_0 - Kd^{-1/2} , \quad (5)$$

where K is a constant, T_0 only depends on the tensile properties and d represents the mean linear intercept between high-angle boundaries. The d-value in steel having AF-microstructure is smaller than the distance d-measured in upper B-microstructure between packets (high-angle boundary existing in this microstructure with a lower probability). These results confirm a beneficial effect of interlocked AF-microstructure [4, 10].

Conclusions

The contribution is devoted to the study of physical metallurgy principles controlling the AF formation. The Ti_2O_3 inclusion nucleability and additional effect of MnS and TiN adhered on Ti-oxides are analysed. The AF-plates are intragranularly nucleated at inclusions, while the intergranular nucleation controls the B-formation. The AF-microstructure is characterised with increased frequency of high-angle boundaries among adjoining plates interfaces. These results confirm the achievement of higher AF-resistance to cleavage crack propagation.

Acknowledgement

The authors acknowledge the Grant Agency of Czech Republic for financial support project No. 106/03/0264.

References:

- [1] BABU, S.S., BADHESIA, H.K.D.K. In *Mater. Sci. Eng.*, 1992, 1, A156.
- [2] BHADSHIA, H.K.D.K. *Bainite in Steels*. London: Inst. of Mater, Cambridge, 1992, 245.
- [3] TAKAMURA, J., MIZOGUCHI, S. Roles of Oxides in Steels Performance – Metall. of Oxides in Steels. In *Proceedings of the 6th Internat. Iron and Steel Congress, ISIJ*. Nagoya, 1990, 591.
- [4] SHIM, J.H., BYUN, J.S., CHO, Y.W., OH, Y.J., SHIM, J.D., LEE, D.N. *ISIJ Internat.*, 2000, 40, 819.
- [5] BYUN, J.S., SHIM, J.H., CHO, I.W., LEE, D.N. *Acta Mater.*, 2003, 51, 1593.
- [6] MAZANCOVÁ, E., JONŠTA, Z., MAZANEC, K. *Acta Metall. Slov.*, 2004, 10, 179.
- [7] CHRISTIAN, J.W. *The Theory of Transform. in Metals and Alloys*, 2nd. Ed., Pergamon Press, Oxford, 1975, 624.
- [8] MADARIAGA, I., GUTIÉRREZ, I. *Acta Mater.*, 1999, 47, 951.
- [9] YAMAMOTO, K., HASEGAWA, T., TAKAMURA, J. *ISIJ Internat.*, 1996, 36, 80.
- [10] GOURGUEZ, A.F., FLEWER, H.M., LINDLEY, T.C. *Mater. Sci. Technol.*, 2000, 16, 26.
- [11] DIAZ-FUENTES, M., IZA-MENDIA, A., GUTUÉRREZ, I. *Metall. Mater. Trans.A*, 2003, 34A, 2525.